International Journal of Engineering, Mathematical and Physical Sciences
ISSN: 2517-9934
Vol:9, No:5, 2015

Chemical and Vibrational Nonequilibrium Hypersonic Viscous Flow around an Axisymmetric Blunt Body

R. Haoui

***Abstract*—**Hypersonic flows around spatial vehicles during their reentry phase in planetary atmospheres are characterized by intense aerothermodynamics phenomena. The aim of this work is to analyze high temperature flows around an axisymmetric blunt body taking into account chemical and vibrational non-equilibrium for air mixture species and the no slip condition at the wall. For this purpose, the Navier-Stokes equations system is resolved by the finite volume methodology to determine the flow parameters around the axisymmetric blunt body especially at the stagnation point and in the boundary layer along the wall of the blunt body. The code allows the capture of shock wave before a blunt body placed in hypersonic free stream. The numerical technique uses the Flux Vector Splitting method of Van Leer. CFL coefficient and mesh size level are selected to ensure the numerical convergence.

***Keywords*—**Hypersonic flow, viscous flow, chemical kinetic, dissociation, finite volumes, frozen and non-equilibrium flow.

I. Introduction

THIS article presents a calculation of viscous flow around an axisymmetric blunt body. In the present work, we employ a numerical technique to simulate the reactive viscous supersonic flow and variation of parameters in the boundary layer thickness on the body surface. The gas considered is the air in a standard state composed of 21% of O_2and79% of N_2which is supposed a perfect gas. The free stream parameters are 170 Pascal and 295K corresponding at the altitude of 45 Km. The flight Mach number is 10. In this case we take into account of the nonequilibrium vibration and dissociation.

The nonlinear partial derivative equations system which governs this flow is solved by an explicit unsteady numerical scheme [1] by the finite volume method [2] for reactive flow [3]. It is clear that the stationary solution obtained depends on the size of the mesh used in the numerical Discretization [4]. We tested convergence for an inviscid flow by using a refining of grid which will enable us to have the exact solution.

II. Governing of Equations

In a Newtonian fluid the viscous stresses are proportional to the rates of deformation. The three-dimensional form of Newton's law of viscosity for compressible flows involves two constants of proportionality, then first dynamic viscosity μ to relate stresses to linear deformations and the second viscosity λ to relate stresses to the volumetric deformation. The viscous stress components are:

$$\tau_{xx} = 2\mu\frac{\partial u}{\partial x} + \lambda\, div(\vec{V})$$

$$\tau_{yy} = 2\mu\frac{\partial v}{\partial y} + \lambda\, div(\vec{V})$$

$$\tau_{zz} = 2\mu\frac{\partial w}{\partial z} + \lambda\, div(\vec{V})$$

$$\tau_{xy} = \tau_{yx} = \mu\left(\frac{\partial u}{\partial y} + \frac{\partial v}{\partial x}\right)$$

$$\tau_{xz} = \tau_{zx} = \mu\left(\frac{\partial u}{\partial z} + \frac{\partial w}{\partial x}\right)$$

$$\tau_{yz} = \tau_{zy} = \mu\left(\frac{\partial v}{\partial z} + \frac{\partial w}{\partial y}\right)$$

Not much is known about the second viscosity λ, because its effect is small in practice. For gases a good working approximation can be obtained by taking the value $\lambda = -\frac{2}{3}\mu$ [5].

The Navier-stokes equations in a flux-vector formulation in Cartesian coordinate system are given by

$$\frac{\partial W}{\partial t} + \frac{\partial E}{\partial x} + \frac{\partial F}{\partial y} + \frac{\partial G}{\partial z} = \Omega \qquad (1)$$

where W, E, F, G and Ω are vectors given by

$$W = \begin{pmatrix} \rho \\ \rho u \\ \rho v \\ \rho w \\ \rho e \\ \rho_s \\ (\rho_s e_{vs})_{O2,N2} \end{pmatrix}$$

$$E = \begin{pmatrix} \rho u \\ \rho u^2 + p - \tau_{xx} \\ \rho uv - \tau_{xy} \\ \rho uw - \tau_{xz} \\ (\rho e + p)u - u\tau_{xx} - v\tau_{xy} - w\tau_{xz} + q_x \\ \rho_s u \\ (\rho_s e_{vs} u)_{O2,N2} \end{pmatrix}$$

$$F = \begin{pmatrix} \rho v \\ \rho uv - \tau_{xy} \\ \rho v^2 + p - \tau_{yy} \\ \rho vw - \tau_{yz} \\ (\rho e + p)v - u\tau_{xy} - v\tau_{yy} - w\tau_{yz} + q_y \\ \rho_s v \\ (\rho_s e_{vs} v)_{O2,N2} \end{pmatrix}$$

R. Haoui is with the Mechanical Engineering Department, University of sciences and technology Houari Boumediene, BP32, Al Alia, Algiers, Algeria (phone:213-21207765; fax: 213-21207765; e-mail: haoui_rabah@yahoo.fr).

$$G = \begin{pmatrix} \rho w \\ \rho uw - \tau_{xz} \\ \rho vw - \tau_{yz} \\ \rho w^2 + p - \tau_{zz} \\ (\rho e + p)w - u\tau_{xz} - v\tau_{yz} - w\tau_{zz} + q_z \\ \rho_s w \\ (\rho_s e_{vs} w)_{O2,N2} \end{pmatrix}$$

$$\Omega = \begin{pmatrix} 0 \\ 0 \\ 0 \\ 0 \\ 0 \\ \omega_{cs} \\ (\omega_{vs})_{O2,N2} \end{pmatrix}$$

The heat flux vector q has three components q_x,q_y and q_z given by the Fourier's law of heat conduction relates the heat flux to the local temperature gradient. So

$$q_x = -k\frac{\partial T}{\partial x}, q_y = -k\frac{\partial T}{\partial y}, q_z = -k\frac{\partial T}{\partial z} \quad (2)$$

where k denotes the coefficient of thermal conductivity, it is function of Prandtl number $Pr = 0.75$, viscosity and specific heat.

$$k = C_p.\mu/Pr \quad (3)$$

The energy e per unit of mass is such as:

$$e = \sum_{s=1}^{5} c_{vs}\, T + \sum_{s=1}^{5} Y_s\, e_{vs} + \sum_{s=1}^{5} Y_s\, h_f^0 + \frac{1}{2}(u^2 + v^2 + w^2) \quad (4)$$

h_f^0 is the enthalpy of formation of the species s in j/kg:

$$h_f^0(O) = 15.43\ 10^6, \quad h_f^0(N) = 33.62\ 10^6$$
$$h_f^0(NO) = 2.996\ 10^6$$
$$h_f^0(O2) = h_f^0(N2) = 0$$

The pressure of the mixture is obtained by the equation of state:

$$p/\rho = r_m T \quad (5)$$

where

$$r_m = \frac{R}{M_m} \quad (6)$$

The temperature of the mixture is calculated by using the energy equation (4). The source term of the chemical equation of evolution of species s evaluated through:

$$\omega_{cs} = M_s \sum_{r=1}^{r} (\upsilon_s'' - \upsilon_s')\, J_r \quad (7)$$

where:

$$J_r = K_f \prod_s \left(\frac{\rho_s}{M_s}\right)^{\upsilon_s'} - K_b \prod_s \left(\frac{\rho_s}{M_s}\right)^{\upsilon_s''} \quad (8)$$

υ_s' and υ_s'' are the stoichiometric coefficients of the reactants and products of species s respectively for each chemical reaction (r) such as:

$$\sum_s \upsilon_s' A_s \overset{K_f, K_b}{\Longleftrightarrow} \sum_s \upsilon_s'' A_s \quad (9)$$

Both forward and backward reaction rates are represented by K_f and K_b. An empirically expression for the forward reaction rate K_f may be written as

$$K_f = A\, T^n\, exp\left(-\frac{T_d}{T}\right) \quad (10)$$

In this equation, the temperature of translation-rotation T is replaced by the geometric average between T and T_v $(T^{1-q}.T_v^q)$ with $q = 0.3$ taking into account the coupling between vibration and dissociation (CVD) according to the Park model [3].

For the backward reaction rate K_b, it is function of the equilibrium constant K_{eq}

$$K_b = \frac{K_f}{K_{eq}} \quad (11)$$

The constants A, n and the temperature characteristic of dissociation T_d are given by Gardiner model [3]. The equilibrium constant of the chemical reaction is given like a polynomial of the 4^{th} degree:

$$K_{eq} = exp(c_0 + c_1 z + c_2 z^2 + c_3 z^3 + c_4 z^4) \quad (12)$$

where $z = 10000/T$, and the coefficients c_0 through c_4 are provided for each reaction [3].

The term of energy production of vibration ω_{vs} is such as:

$$\omega_{vs} = \rho_s \frac{e_{vs}(T) - e_{vs}(T_v)}{\tau_s} + e_{vs}(T_v).\omega_{cs} \quad (13)$$

$e_{vs}(T_v)$ is the energy at the temperature of vibration T_v and $e_{vs}(T)$ is the equilibrium energy of vibration at the temperature T of translation-rotation expressed as:

$$e_v(T) = \frac{r\,\theta_v}{exp\left(\frac{\theta_v}{T}\right) - 1} \quad (14)$$

r is the constant of a particular gas and θ_v is the temperature characteristic of vibration for each molecule. In the present work, we take:

$$\theta_{vO2} = 2239K,\ \theta_{vN2} = 3354K,\ \theta_{vNO} = 2720K \quad (15)$$

The time characteristic of vibration of a species s in the mixture τ_s is function of the temperature, the pressure and the molar fractions X_i. It can be calculated as [3]:

$$\frac{1}{\tau_s} = \sum_i \frac{X_i}{\tau_{s,i}} \quad (16)$$

where $s = O_2, N_2$ and $i = O_2, N_2, NO, O, N$. $\tau_{s,i}$ is the time characteristic of vibration of the species s in a mixture containing species i. We have:

$$\tau_{O2,O2} = \frac{1.692\ 10^{-9}}{p}\ exp\left(101.44\ T^{-1/3}\right) \quad (17)$$

$$\tau_{N2,N2} = \frac{1.1\ 10^{-11}}{p}\ T^{1/2}\ exp\left(154.0\ T^{-1/3}\right) \quad (18)$$

Experiments for binary exchanges, made it possible to evaluate vibrational relaxation time of O_2 in monatomic oxygen [8] and of N_2 in O [9]. The pressure p is in atmospheres and τ in seconds.

$$\tau_{O2,O} = \frac{T^{2/3}}{p}\, exp\left(55.2\, T^{-1/3} - 26.95\right) \quad (19)$$

$$\tau_{N2,O} = \frac{T^{2/3}}{p}\, exp\left(70.3\, T^{-1/3} - 24.35\right) \quad (20)$$

To determine the relaxation times which are not given by the experimental correlations is supposed that the relaxation time of a species s is same whatever the species i which it meets, provided that their masses are identical. Therefore, the following approximations can be employed:

$$\begin{gathered}\tau_{O2,N} \cong \tau_{O2,O} \;;\; \tau_{N2,N} \cong \tau_{N2,O} \\ \tau_{O2,N2} \cong \tau_{O2,NO} \cong \tau_{O2,O2} \\ \tau_{N2,O2} \cong \tau_{N2,NO} \cong \tau_{N2,N2}\end{gathered} \quad (21)$$

The model with 17 reactions is:

O_2+M ↔ 2O+M	r = 1 to 5
N_2+M ↔ 2N+M	r = 6 to 10
NO+M ↔ N+O+M	r = 11 to 15
N_2+O ↔ NO+N	r =16
NO+O ↔ O_2+N	r = 17

The species Mcan be one of the five chemical species (in the order: $O_2, N_2, NO, O\ or\ N$).

III. Axisymmetric Formulation

A method developed within the Sinus project of the INRIA Sophia-Antipolis [1] makes it possible to pass from 3D to 2D axisymmetric by using a technique of disturbance of domain. Taking advantage of this finding, here the problem is considered as being axisymmetric.

The system of (1) can be written as:

$$mes(C_{i,j})\frac{\partial W_{i,j}}{\partial t} + \sum_{a\in\{x,x',y,y'\}}\left(F_{i,j}\vec{\imath} + G_{i,j}\vec{\jmath}\right).\overrightarrow{\eta_a} - H.aire(C_{i,j}) = \Omega \quad (22)$$

$mes(C_{i,j})$ is the measurement (in m^3) of an infinitely small volume of center (i,j), $aire(C_{i,j})$ is the surface of the symmetry plane passing by the center of elementary volume and η_a is the integrated normal. The third term of the equation expresses the axisymmetric flow condition. The new Fluxes W, F, G and H becomes [6]:

$$W = \begin{pmatrix} \rho \\ \rho u \\ \rho v \\ \rho e \\ \rho_s \\ (\rho_s e_{vs})_{O2,N2} \end{pmatrix}$$

$$F = \begin{pmatrix} \rho u \\ \rho u^2 + p - \tau_{xx} \\ \rho uv - \tau_{xy} \\ (\rho e + p)u - u\tau_{xx} - v\tau_{xy} + q_x \\ \rho_s u \\ (\rho_s e_{vs} u)_{O2,N2} \end{pmatrix}$$

$$G = \begin{pmatrix} \rho v \\ \rho uv - \tau_{xy} \\ \rho v^2 + p - \tau_{yy} \\ (\rho e + p)v - u\tau_{xy} - v\tau_{yy} + q_y \\ \rho_s v \\ (\rho_s e_{vs} v)_{O2,N2} \end{pmatrix}$$

$$H = \begin{pmatrix} 0 \\ -2\tau_{xy} \\ 2p - 2\tau_{yy} \\ -2u\tau_{xy} - 2v\tau_{yy} + 2v\tau_{zz} + 2q_y \\ 0 \\ 0 \end{pmatrix}$$

$$\Omega = \begin{pmatrix} 0 \\ 0 \\ 0 \\ 0 \\ \omega_{cs} \\ (\omega_{vs})_{O2,N2} \end{pmatrix}$$

where

$$\tau_{xx} = 2/3\mu\left(2\frac{\partial u}{\partial x} - \frac{\partial v}{\partial y}\right)$$

$$\tau_{xy} = \tau_{yx} = \mu\left(\frac{\partial u}{\partial y} + \frac{\partial v}{\partial x}\right)$$

$$\tau_{yy} = 2/3\mu\left(2\frac{\partial v}{\partial y} - \frac{\partial u}{\partial x}\right)$$

$$\tau_{xz} = \tau_{zx} = 0$$

$$\tau_{zz} = 2/3\mu\left(-\frac{\partial u}{\partial x} - \frac{\partial v}{\partial y}\right)$$

$$\tau_{yz} = \tau_{zy} = 0$$

IV. Discretization in Time

The present numerical method is based on an explicit approach in time and space. The step of time Δt is such as:

$$\Delta t_{i,j} = min\left[\left(\frac{\Delta x.CFL}{\|V\|+a}\right), \left(\frac{(\Delta x)^2.CFL}{2\mu/\rho}\right)\right] \quad (23)$$

The CFL (Courant, Friedrich, Lewis) is a stability factor [4], V is the velocity of the flow,a the speed of sound and Δx is the small length of the mesh at the same point (i,j). At each time step and for each point(i,j), the system of (22) can be written as:

$$W_{i,j}^{n+1} = W_{i,j}^{n} - \frac{\Delta t_{i,j}}{mes(C_{i,j})}\sum_{a\in\{x,x',y,y'\}}\left({F_{i,j}}^{n}\vec{\imath} + {G_{i,j}}^{n}\vec{\jmath}\right)\overrightarrow{\eta_a} + \Delta t_{i,j}\frac{aire(C_{i,j})}{mes(C_{i,j})}{H_{i,j}}^{n} + \Delta t_{i,j}\,{\Omega_{i,j}}^{n} \quad (24)$$

The choice of the grid and CFL plays an important role to obtain the stationary solution.

V. Decomposition of Van-Leer

In this study, the decomposition of Van-Leer [7] is selected, namely a decomposition of flows in two parts f_{VL}^{-} and f_{VL}^{+}. This decomposition must apply to the present two-dimensional problem by calculating the flow within each interface between two cells. Moreover, through this interface, the normal direction is paramount, thus, a change of reference mark is

applied to place in the reference mark of the interface and its normal by the intermediary of a rotation R, Fig. 1.

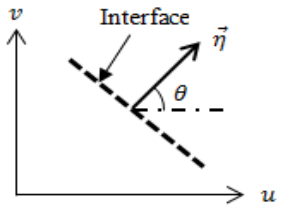

Fig. 1 Interface and its normal

The vector W_E (variable of Euler) is written W_E^R in the new reference mark

$$W_E^R = \begin{pmatrix} \rho \\ \rho\overrightarrow{V_n} \\ \rho\, e \end{pmatrix} \tag{25}$$

where $\overrightarrow{V_n}$ is obtained from $\vec{V}$, via the rotation R, in the following way:

$$\vec{V} = \begin{pmatrix} u \\ v \end{pmatrix} \rightarrow \vec{V}_n = \begin{pmatrix} u_n \\ v_n \end{pmatrix} = \begin{pmatrix} cos\,\theta & sin\,\theta \\ -sin\,\theta & cos\,\theta \end{pmatrix}\begin{pmatrix} u \\ v \end{pmatrix} \tag{26}$$

where

$$cos\,\theta = \frac{\eta_x}{\|\vec{\eta}\|}, \quad sin\,\theta = \frac{\eta_y}{\|\vec{\eta}\|} \tag{27}$$

$$\|\vec{\eta}\| = \sqrt{\eta_x^2 + \eta_y^2} \tag{28}$$

The overall transformation R is written overall

$$R = \begin{pmatrix} cos\,\theta & sin\,\theta \\ -\,sin\,\theta & cos\,\theta \end{pmatrix} \tag{29}$$

$$R^{-1} = \begin{pmatrix} cos\,\theta & -sin\,\theta \\ sin\,\theta & cos\,\theta \end{pmatrix} \tag{30}$$

Moreover, at each interface $i+1/2$, two neighbor states i and $i+1$ are known. Thus, one can calculate the one-dimensional flow F through the interface, total flow $f(W,\eta)$ being deduced from F by applying the opposite rotation, as:

$$f(W,\vec{\eta}) = \|\vec{\eta}\|.R^{-1}\big(F(W^R)\big) \tag{31}$$

This property makes it possible to use only one component of flow f (F for example) to define the decomposition of flow in two dimensions. Moreover, this method is much easy and simple to implement than the decomposition of flow in two dimensions $f = F\eta_x + G\eta_y$.

The expressions of F_{VL}^+ and F_{VL}^- in 1-D, which are those of $F_{VL}^+(W^R)$ and $F_{VL}^-(W^R)$ by rotation R, where W^R is defined like the transform of W, can be written in the following from:

$$F_{VL}^+(W^R) = \begin{cases} F(W^R) & M_n \geq 1 \\ \begin{pmatrix} \frac{\rho a}{4}\left(\frac{u_n}{a}+1\right)^2 = f_1^+ \\ \frac{f_1^+}{\gamma}[(\gamma-1)u_n + 2a] \\ f_1^+ . v_n \\ \frac{f_1^+}{2}\left[\frac{((\gamma-1)u_n+2a)^2}{\gamma^2-1} + v_n^2\right] \end{pmatrix} & |M_n| < 1 \\ 0 & M_n \leq -1 \end{cases} \tag{32}$$

$$F_{VL}^-(W^R) = \begin{cases} 0 & M_n \geq 1 \\ \begin{pmatrix} \frac{\rho a}{4}\left(\frac{u_n}{a}-1\right)^2 = f_1^- \\ \frac{f_1^-}{\gamma}[(\gamma-1)u_n - 2a] \\ f_1^- . v_n \\ \frac{f_1^-}{2}\left[\frac{((\gamma-1)u_n-2a)^2}{\gamma^2-1} + v_n^2\right] \end{pmatrix} & |M_n| < 1 \\ F(W^R)M_n & \leq -1 \end{cases} \tag{33}$$

where $M_n = u_n/a$, u_n and v_n are the velocity in the reference mark of the interface.

VI. Boundary Conditions

Boundary conditions give the most serious problems for the designer of general purpose CFD codes. All CFD problems are defined in terms of initial and boundary conditions. It is important to specify these correctly and understands their role in the numerical algorithm. In unsteady problems the initial values of all flow variables need to be specified at all points in the computational domain. The present work describes the implementation of the following most common boundary conditions in the discredited equations of the finite volume method: inlet, outlet, wall and symmetry Fig. 2.

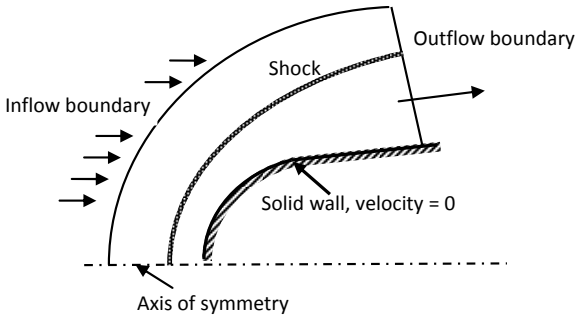

Fig. 2 Computational domain and boundary conditions

A. Inlet Boundary Conditions

At the inlet the Mach number, pressure and temperature are fixed because the flow is hypersonic.

B. Body Surface

The no-slip condition for the velocity is usually used at the body surface. The temperature gradient at the wall is zero, in accordance with the Fourier equation of heat conduction in the normal-direction together with the assumption of zero heat flux at the wall, it is the adiabatic wall. No condition is imposed on the wall temperature. In this study, the wall shear stress is calculated by:

$$\tau_w = \mu\left(\frac{\partial V_t}{\partial n}\right)_{wall} = \mu\frac{V_t}{\Delta n} \tag{34}$$

where

$$V_t = \vec{V}.\vec{t} \quad (35)$$

and

$$\Delta n = \sqrt{\Delta x^2 + \Delta y^2} \quad (36)$$

Here we assume that the coordinate of the unit vector $\vec{t}$ is in the direction of the shear force at the wall and the unit vector $\vec{n}$ is normal at $\vec{t}$, Fig. 3.

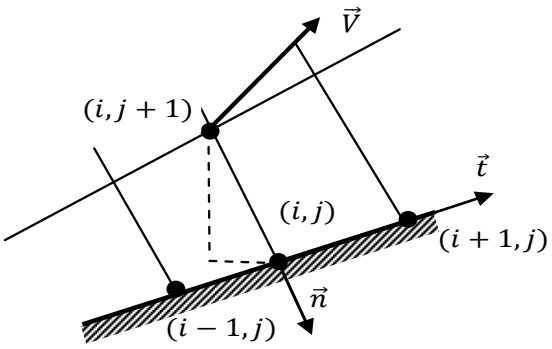

Fig. 3 Grid near the wall

C. Axis of Symmetry

The conditions at axis of symmetry boundary are no flow and no scalar flux across the axis.

D. Outlet Boundary Conditions

At the exit of the computational domain, the values of the flow parameters are extrapolated from the interior values, including in the boundary layer.

VII. Results and Interpretations

Consider an axisymmetric blunt body defined geometrically by hemisphere as shown in Fig. 4, when the ray is denoted by $r = 4\ cm$. The computational domain is limited by the blunt body and an ellipse with $a = 1.2\,r$ and $b = 1.5\,r$. Assume a hypersonic flow-field where the free-stream Mach number equal 10, corresponding to the velocity of 3442 m/s. The configuration is at zero degree angle of attack. A $(20x101)$ grid system is created by an elliptic scheme, 20 meshes along the axis and 101 meshes along the wall. Note that grid points are clustered near the stagnation region where the flow is expected to the subsonic. In our calculations we used several sizes of grid while starting with that of Fig. 4 (20x101). The grid (70x356) is selected since it gives good results and requires less time computing where we stop calculations when the residue equal 10^{-5} .

Fig. 5 shows the velocity profile at the station $x/r = 0.893$. We observe clearly the boundary layer thickness where $\frac{\eta}{r} \approx 0.1$. We can also observe the detached shock and the free stream.

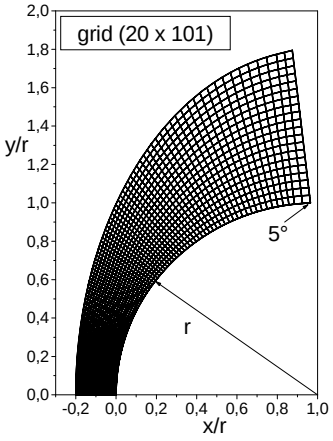

Fig. 4 Grid of solution domain

The thermal boundary layer is shown in Fig. 6. We give also the temperature of vibration of O_2 and N_2. The thermal boundary layer thickness is about $\eta/r \approx 0.1$, the temperature of translation-rotation at the wall is equal to 4447K and the ones of vibration for O_2 and N_2 are $4173K$ and $3234K$ respectively. The difference is explained by the fact that the flow is in nonequilibrium. It is observed that the shock through the vibration temperature does not vary suddenly, the relaxation time of the temperature T is less than the relaxation time of vibration temperature. Chemical reactions will also take place in the boundary layer as the temperature T varies considerably. Figs. 7 and 8 shows the mass fractions variations of (O_2, N_2) and (NO, O, N) respectively.

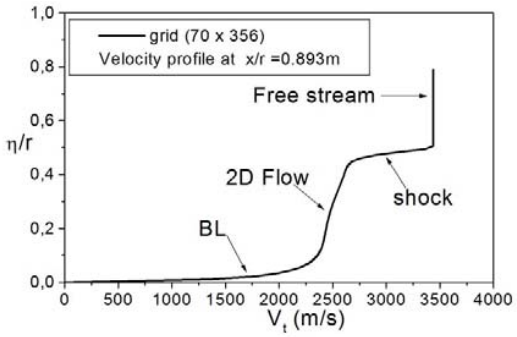

Fig. 5 Velocity profile at $x/r = 0.893$

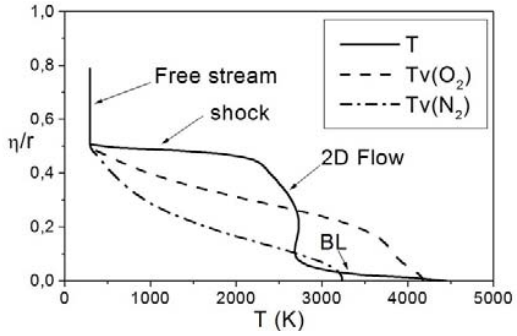

Fig. 6 Velocity profile at $x/r = 0.893$

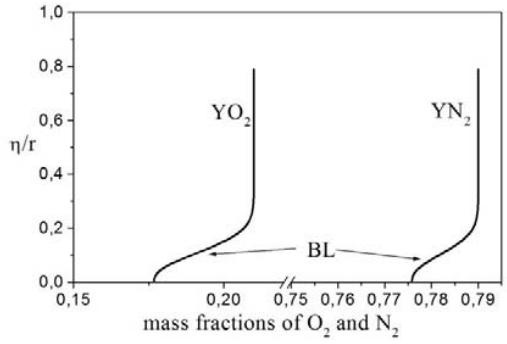

Fig. 7 Mass fractions at $x/r = 0.893$

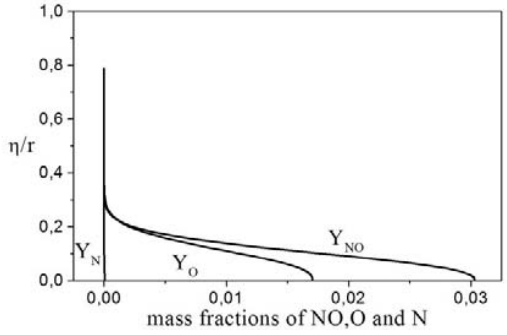

Fig. 8 Mass fractions at $x/r = 0.893$

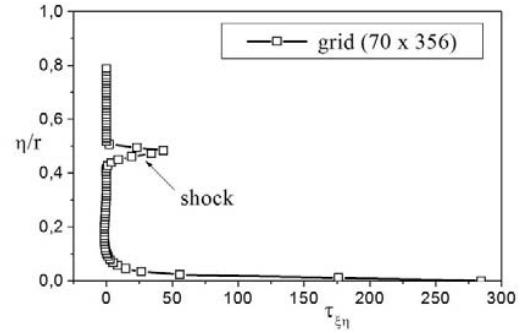

Fig. 9 Stress viscous flow at $x/r = 0.893$

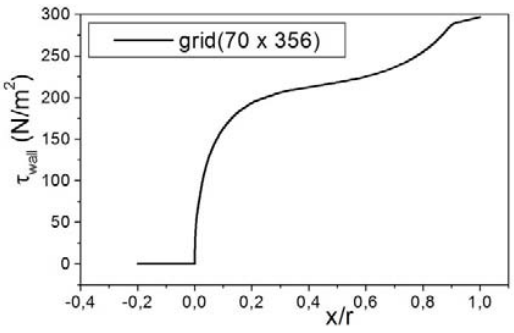

Fig. 10 Shear stress along the wall

Another parameter very significant to calculate in this kind of flow, it is that of the stress τ_{xy}. Fig. 9 shows the variation of the stress along the normal of the wall at $x/r = 0.893$. This profile itself converges to the exact solution for a grid of $(70x356)$. It is observed that the intensity of the stress increases quickly while approaching the wall. The viscous stress at the wall can be calculated from the all stresses at the same point. Fig. 10 shows the variation of the stress τ_{wall}along the wall of the blunt body.

The variation of other parameters such as pressure, temperature and density from free stream until the stagnation point along the axis and along the wall is given by Figs. 11-13. Concerning the pressure, it increases rapidly through the shock and it continues to increase until the stagnation point when takes the value of $P/P_a = 149.24$ then decreases along the wall. As against the temperature after its increase through the shock when its value is $T/T_a = 20.16$, it decreases until the stagnation point when it will have the value of $T/T_a = 16.47$. This decrease is caused by the dissociation of air in five species. It is the endothermic reactions. Along the wall, the temperature remains almost constant. The density follows the same variation as the pressure. In the three figures the shock position is $x/r = -0.11$. Fig. 14 shows the evolution details of the mass fractions. Chemical reactions begin after the shock gradually until stagnation point where we are 13.85% of O_2, 75.74% of N_2, 6.91% of NO, 3.47% of O and 0.034% of O, and then the mass fractions of NO, O and N decrease slowly along the wall and those of O_2 and N_2 increase.

Finally, we give the overall representation of the flow as iso-contours for all variables around the blunt body, Figs. 15-24. A comparison of Mach-contours with the inviscid flow is represented on Figs. 16 and 17. It is completely clear that the boundary layer influences on the flow parameters.

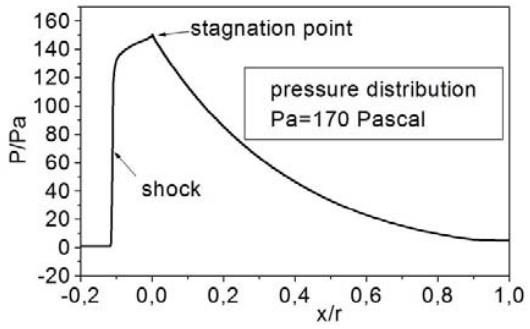

Fig. 11 Pressure distribution

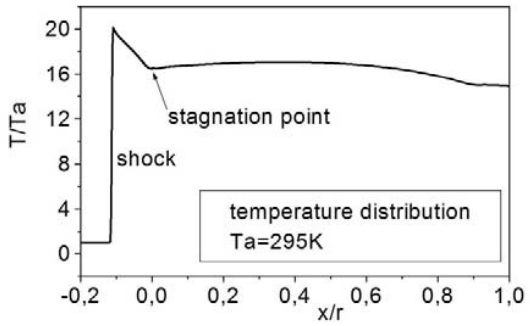

Fig. 12 Temperature distribution

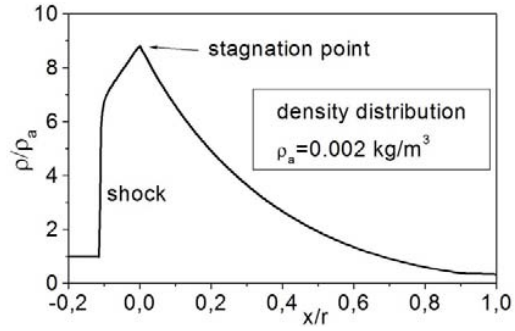

Fig. 13 Density distribution

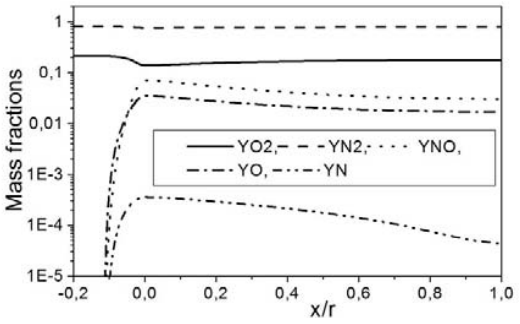

Fig.14 Mass fractions distribution

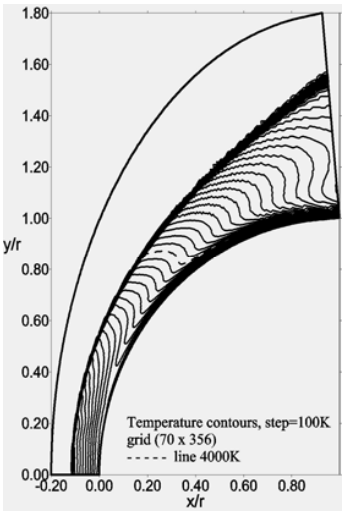

Fig. 15 Temperatures contours

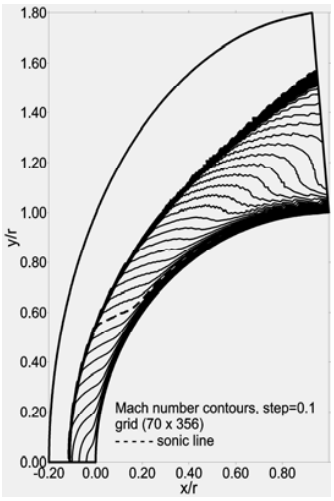

Fig. 16 Mach number contours for viscous flow

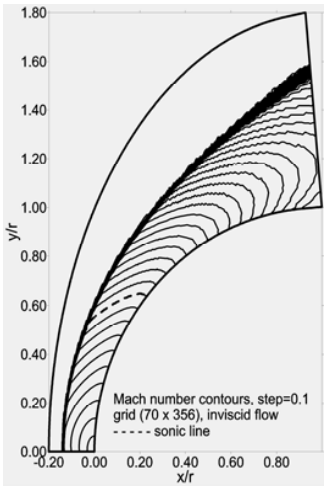

Fig. 17 Mach number contours for inviscid flow

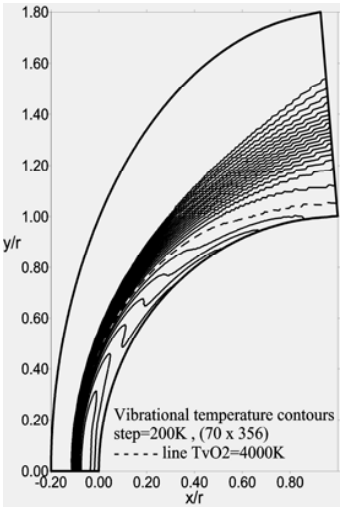

Fig. 18 Vibrational temperature contours of O_2

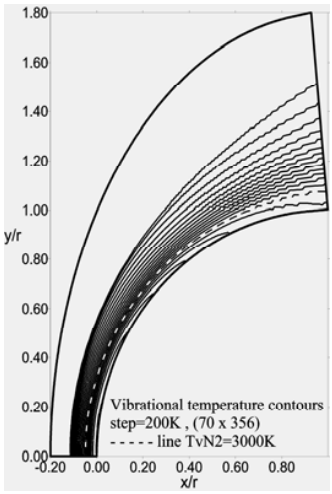

Fig. 19 Vibrational temperature contours of N_2

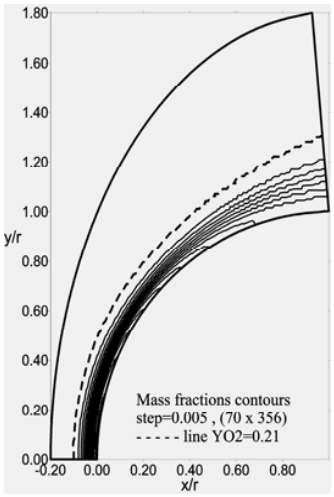

Fig. 20 Mass fraction contours of O_2

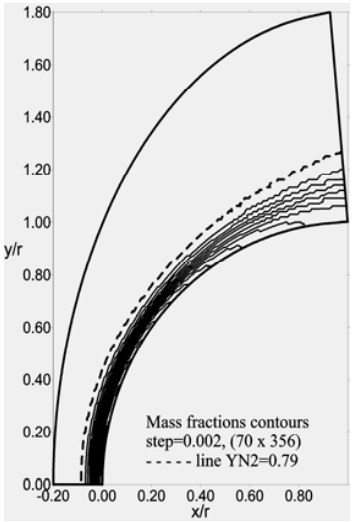

Fig. 21 Mass fraction contours of N_2

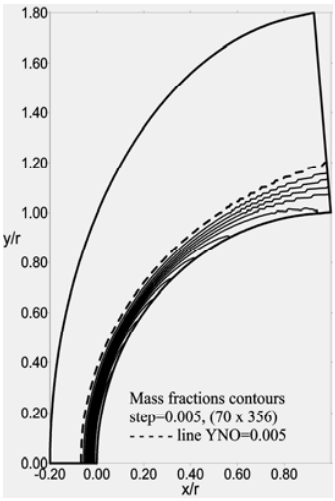

Fig. 22 Mass fraction contours of NO

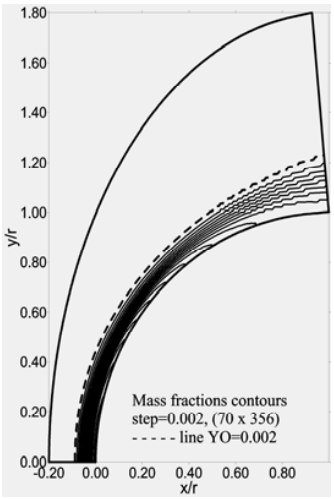

Fig. 23 Mass fraction contours of O

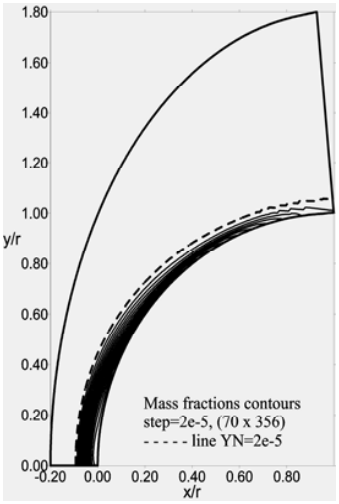

Fig. 24 Mass fraction contours of N

VIII. Conclusion

The numerical simulation of the flows around blunt bodies at high temperature provided satisfactory results from a numerical and a physical point of view. With high degree of accuracy requirements, computational convergence is achieved and the physical phenomena considered are visible after the detached shock wave and around the blunt body. The study of the reactive flow around a blunt body is more realistic if we take into account the effect of viscosity. Navier-Stokes equations give a more explanatory solution to the phenomena occurring near the adiabatic wall. The temperature at the wall is very high compared to the case Euler where did not take into account of the non-slip condition [3].

References

[1] A. Goudjo, J.A. Désidéri, "a finite volume scheme to resolution an axisymmetric Euler equations," Research report INRIA 1005, 1989.
[2] R. Haoui, A. Gahmousse, D. Zeitoun, "Chemical and vibrational nonequilibrium flow in a hypersonic axisymmetric nozzle," International Journal of Thermal Sciences, article n° 8, volume 40, (2001), pp787-795.
[3] R. Haoui, "Finite volumes analysis of a supersonic non-equilibrium flow around the axisymmetric blunt body," International Journal of Aeronautical and space Sciences, 11(2), (2010), pp59-68.
[4] R. Haoui, A. Gahmousse, D. Zeitoun, "Condition of convergence applied to an axisymmetric reactive flow," 16th CFM, n°738, Nice, France, 2003.
[5] K. A Hoffmann, "Computational fluid dynamics for engineers, «Volume II" Library of congress Catalog, March **1**995, ISBN 0-9623731-8-4.
[6] R. Haoui, "Effect of mesh size on the supersonic viscous flow parameters around an axisymmetric blunt body," International Journal of Mechanical, Aerospace, Industrial and Engineering, 8(7),(2014), pp1263-1268.
[7] B. Van Leer, "Flux Vector Splitting for the Euler Equations," Lecture Notes in Physics. 170, (1982), 507-512.
[8] J.H. Kiefer, and R.W. Lutz, "The effect of Oxygen atoms on the vibrational relaxation of Oxygen," 11th Symposium on combustion. Pittsburg, (1967), 67-74.
[9] W.D. Brashears, P.F. Bird, "Effects of Oxygen atoms on the vibrational relaxation of Nitrogen," The journal of chemical physics, 48 (10) (1968).